

Submillimetre observations of $z > 6$ quasars

Ian Robson¹, Robert S. Priddey^{2,3}, Kate G. Isaak⁴, Richard G. McMahon⁵

¹ *UK Astronomy Technology Centre, Blackford Hill, Edinburgh EH9 3HJ, UK*

² *Imperial College, Blackett Laboratory, Prince Consort Road, London SW7 2BZ, UK*

³ *Department of Physics, Astronomy & Mathematics, University of Hertfordshire, College Lane, Hatfield AL10 9AB, UK*

⁴ *School of Physics & Astronomy, University of Wales - Cardiff, Cardiff, CF24 3YB, UK*

⁵ *Institute of Astronomy, Madingley Road, Cambridge, CB3 0HA, UK*

Submitted 15th February, 2004; Accepted 15th April, 2004

ABSTRACT

We report on submillimetre (submm) observations of three high redshift quasars ($z > 6$) made using the SCUBA camera on the James Clerk Maxwell Telescope (JCMT). Only one of the sample was detected ($> 10\sigma$ significance) at $850\mu\text{m}$ – SDSS J1148+5251 ($z = 6.43$). It was also detected at $450\mu\text{m}$ ($> 3\sigma$ significance), one of the few quasars at $z > 4$ for which this has been the case. In combination with existing millimetric data, the $850\mu\text{m}$ and $450\mu\text{m}$ detections allow us to place limits on the temperature of the submm-emitting dust. The dust temperature is of no trivial importance given the high redshift of the source, since a cold temperature would signify a large mass of dust to be synthesized in the little time available (as an extreme upper limit in only 0.9Gyr since $z = \infty$). We find, however, that the combined millimetre and submm data for the source cannot simply be characterised using the single-temperature greybody fit that has been used at lower redshifts. We discuss the results of the observing and modelling, and speculate as to the origin of the deviations.

Key words:

quasars:general-galaxies:high-redshift-submillimetre-dust

1 INTRODUCTION

A number of independent lines of investigation over the last 10 years have placed submillimetre (submm) observations of high-redshift quasars into the spotlight. Observations have unveiled a population of extremely luminous submm sources lying at high redshift, believed to be the dust-obscured, star-forming ancestors of massive elliptical galaxies. Contemporaneously, it was realised that a tight correlation exists between the stellar velocity dispersion of galactic spheroids, and the mass of their central, supermassive black hole (Gebhardt et al. 2000). Taken together, these indicate that luminous active galactic nuclei (AGN) at high redshift—the build-up phase of a supermassive black hole — are prime sites at which to search for the dust-enshrouded star-burst phase through which, according to the new galaxy-formation paradigm, their massive spheroids necessarily must pass.

The high, sustained luminosity of quasars across the electromagnetic spectrum, allows them to be studied over a wide range of both redshift and observing wavelength. Early observations of $z \sim 4.5$ quasars by McMahon et al. (1994), and Isaak et al. (1994) established that some high redshift quasars were prodigious far infrared emitters with $L_{\text{fir}} \sim 10^{13-14} L_{\odot}$ and estimated masses of cool dust of $\sim 10^{8-9} M_{\odot}$.

The discovery of quasars at $z > 6$ (Fan et al. 2003) now makes it possible to compile homogeneous, well-defined samples over a significant span of the lifetime of the cosmos, from recent times

to the threshold of reionization. Follow-up is simplified by the accurately-known optical positions and the spectroscopic redshifts of the host galaxies, which can readily be determined to the precision required to pinpoint emission lines from molecular gas—a key indicator of the conditions required for star formation.

Recent SCUBA studies of the submm emission from high redshift ($z > 4$), radio-quiet quasars have been reported by McMahon et al. (1999), Isaak et al. (2002) and Priddey et al. (2003b), along with a sample at lower redshift ($z \sim 2$) by Priddey et al. (2003a). A considerable fraction of the targets have been shown to be luminous submm sources. Interestingly, this fraction appears to have no significant dependence upon redshift. Similar conclusions have been drawn from observations at millimetre (mm) wavelengths (eg. Omont et al. (2001), Carilli et al. (2001)).

2 OBSERVATIONS

2.1 The Sample

Our source-list comprised three of the $z \geq 6$ quasars identified by the Sloan Digital Sky Survey team, and reported in Fan et al. (2003). Source parameters are given in Table 1. Observations of the other two quasars known (as of January, 2003) to be at $z > 6$, SDSS J1030+0534 ($z = 6.28$) and SDSS J1306+0356 ($z = 5.99$), have been reported in Priddey et al. (2003b).

2.2 Observations and Data Analysis

Sources were observed using SCUBA (Holland et al. 1999) on the JCMT¹ on the nights of 2003 January 31 and February 01 (UT). Simultaneous observations were made at 850 and 450 μm using photometry mode (placing the source on the central bolometers H7, C14 of the two arrays respectively) with a 60 arcsec azimuth chop at 7.8Hz. Data were taken in groups of 40 samples, with observations repeated until $S_{850\mu\text{m}} \leq 2\text{mJy}$ was achieved. Telescope pointing was checked hourly, and found to be better than 3 arcsec. Mars and Uranus, along with IRC+10216, were used as primary and secondary calibrators respectively. The derived, mean, flux conversion factors were $213 \pm 5\text{Jy/V}$ (850 μm) and $355 \pm 15\text{Jy/V}$ (450 μm), with a variation of $< 10\%$ seen over the course of the observing period. The sky opacity was measured using sky-dips and the recently commissioned water vapour radiometer that measures the direct line-of-sight atmospheric extinction.

Observing conditions on both nights were moderately good, with $0.1 < \tau_{850}^{\text{zen}} < 0.23$ and $0.27 < \tau_{850}^{\text{zen}} < 0.32$ (zenith atmospheric transmission at 850 μm between 79 – 90% and 72 – 76%) respectively. Data were reduced using both the semi-automated ORAC-DR pipeline data reduction package (Jenness & Economou 1999) and a custom reduction procedure based on a series of routines taken from the SURF reduction package (Jenness & Lightfoot 1998a,b). In each case, the final flux represents the weighted (by the individual rms) average taken of all data for a particular source/filter combination.

The initial analysis of the SDSS J1148+5251 dataset revealed considerable variation between both the flux and rms of the individual 40-sample data groups. One explanation of this discrepancy was revealed upon the subsequent publication of a MAMBO-2 image of SDSS J1148+5251 by Bertoldi et al. (2003). It seemed feasible that our fixed, azimuth chop had placed the off-source position over a second, millimetre-bright source in the quasar field during the latter stages of our observation. In order to eliminate this possibility, we therefore obtained subsequent SCUBA photometry on SDSS J1148+5251, in UK service time during the nights of 2003 July 9th, 10th and 12th. This time, a specified chop throw, and position angle fixed relative to RA–Dec, were chosen to avoid the potential contaminant sources. The atmospheric extinction during the observing period was low (with $0.14 < \tau_{850\mu\text{m}}^{\text{zenith}} < 0.19$) and the sky stable. Guided by these new, more reliable and consistent observations, we reanalysed the initial datasets, testing alternative explanations for their disagreement.

3 RESULTS AND DISCUSSION

The measured flux densities of the three sources are tabulated in Table 1, along with the observational parameters of the three sources. For comparison, the mm fluxes, taken from Bertoldi et al. (2003), have also been included. In all cases the numbers in brackets are the 1σ rms values.

Tabulated in Table 2 are the derived 850 μm /1.2mm and 450/850 μm flux ratios for the sample where sufficient data exist. The superscripts and subscripts in columns 4 and 5 give the 1σ upper and lower values of the flux ratios. Also listed are the equivalent

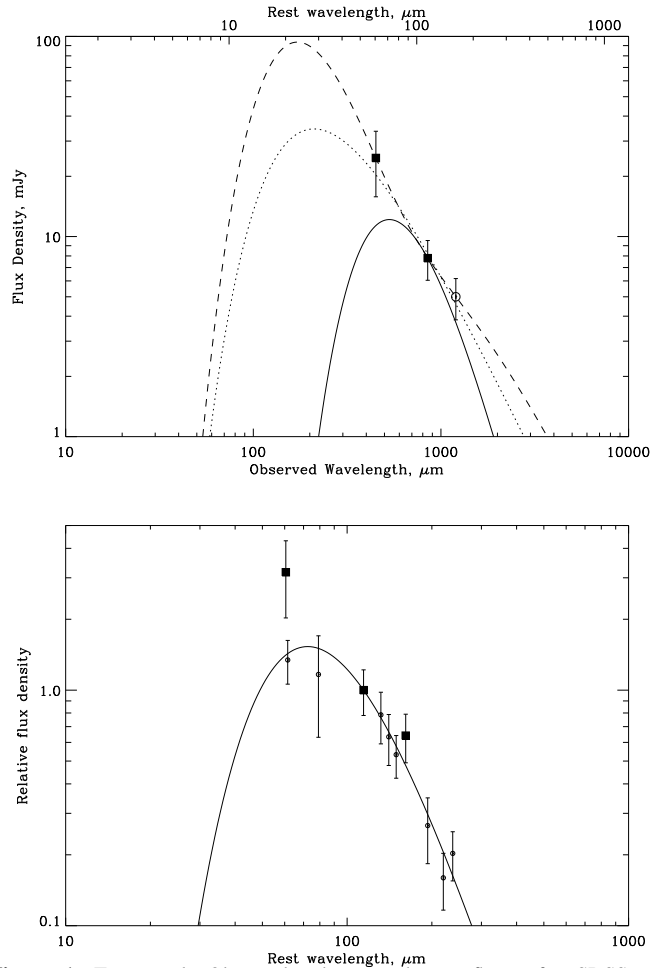


Figure 1. Top panel: Observed submm and mm fluxes for SDSS J1148+5251. Note that for each point, the plotted error bars are the square root of the sum of the squares of the radiometric rms and systematic calibration errors. Superposed over the points are three model SEDs: the solid locus traces the isothermal dust model of $T=40\text{K}$, $\beta = 2.0$ derived by Priddey & McMahon (2001) from a sample of mm and submm observations of $z > 4$ quasars, and fit here through the 850 μm flux; the dotted line traces the SED of a single-temperature dust model with $T_D = 180\text{K}$, $\beta = 0$; the dashed line traces a two-component fit using (T_D, β) of (140, 1.5) and (40, 0). The two-component model is included for illustrative purposes only, as the number of independent data points is smaller than the number of independent constraints on the model.

Bottom panel: A plot of the Priddey & McMahon (2001) SED superposed onto the observed mm and submm data fluxes for SDSS J1148+5251 (filled squares) and BR B1202–0725 (open circles), redshifted to the quasar rest frame. The observed fluxes have been normalised to the 850 μm values appropriate to the individual sources.

numbers for the fiducial single-temperature SED model of a quasar at the mean redshift of the $z > 6$ sample, $\bar{z} = 6.24$, based on a fit to a sample of $z > 4$ quasars by Priddey & McMahon (2001).

3.1 Individual Sources

SDSS J1630+4012 ($z=6.05$) Not detected in either the 850 μm or 450 μm filters; also undetected at 1.2mm.

SDSS J1048+4637 ($z=6.23$) Detected at neither 850 μm nor 450 μm . Based on the detection at 1.2mm (Bertoldi et al. 2003), the SCUBA 850 μm limit is deep enough that we should have been able to detect the source with a 4σ significance were its emission at 1.2mm to be characteristic of a greybody at $T_D = 40\text{K}$. Our

¹ The James Clerk Maxwell Telescope is operated by the Joint Astronomy Centre in Hilo, on behalf of the parent organisations of the Particle Physics and Astronomy Research Council in the UK, the National Research Council of Canada and the Netherlands Organisation for Scientific Research

Table 1. Summary of the source parameters of the SCUBA photometry observations

Source	Redshift	M_B	RA (J2000)	Dec (J2000)	$S_{1.2mm}$ (mJy)	Number of integrations	$S_{850\mu m}$ (mJy)	$S_{450\mu m}$ (mJy)
(1)	(2)	(3)	(4)	(5)	(6)	(7)	(8)	(9)
SDSS J1048+4637	6.23	-28.15	10 48 45.05	+46 37 18.3	3.0(0.4)	120	2.3(2.2)	7.6(11.7)
SDSS J1148+5251	6.43	-28.42	11 48 16.64	+52 51 50.3	5.0(0.6)	600	7.8(0.7)	24.7(7.4)
SDSS J1630+4012	6.05	-26.71	16 03 33.90	+40 12 09.6	$3\sigma < 1.8$	280	2.7(1.9)	15.4(9.6)

Positions and optical magnitudes have been taken from Fan et al. (2003); 1.2mm MAMBO-2 data have been taken from Bertoldi et al. (2003)

Table 2. Summary of quantities derived from submm and optical photometry. See text for an explanation of the quantities and notes on their derivation.

Source	z	M_B	$S_{850\mu m}/S_{1.2mm}$	$S_{450\mu m}/S_{850\mu m}$	$t(\text{inf}) - t(z)$ (Gyr)	M_d ($10^8 M_\odot$)	M_* (min) (M_\odot/yr)	L_{FIR} ($10^{13} L_\odot$)	M_{bh} ($10^9 M_\odot$)	\dot{M}_{acc} (M_\odot/yr)
(1)	(2)	(3)	(4)	(5)	(6)	(7)	(8)	(9)	(10)	(11)
SDSS J1048+4637	6.23	-28.15	< 3.4	—	0.94	< 4.6	< 50	< 0.9	6.0	130
SDSS J1148+5251	6.43	-28.42	$1.6_{1.3}^{1.9}$	$3.2_{2.0}^{4.5}$	0.90	5.3	60	1.1	7.7	170
SDSS J1630+4012	6.05	-26.71	—	—	0.97	< 4.5	< 45	< 0.9	1.6	35
Mean quasar	6.24	-27.76	2.13	1.65	0.94	—	—	—	4.2	90

non-detection thus suggests that the dust in this object is colder than 40K.

SDSS J1148+5251 ($z=6.43$) The most optically luminous of the three sources, detected at both $850\mu m$ and $450\mu m$ with fluxes of $7.8(0.7)\text{mJy}$ and $24.7(7.4)\text{mJy}$ respectively – one of very few quasars at $z > 4$ where this has been achieved. The observed fluxes are not consistent with a Priddey & McMahon (2001) single-temperature SED as can be seen in Figure 1. This can be seen more clearly in Figure 2 a–c, where the $850\mu m/1.2\text{mm}$ and $450/850\mu m$ ratios have been plotted as a function of redshift, both for the single-temperature model (locus) and for a selection of high- z quasars, including those observed in this sample. The observed flux ratios are discrepant at the 1σ level, however are well within the 2σ limits.

3.2 Observed Fluxes

The three sources observed show quite different submm properties, in spite of their similar absolute B-band (M_B) magnitudes (column [3] in Table 2), and so inferred blackhole/bulge masses (see column [10] in Table 2). This is not surprising as, to date, it has not been possible to establish a correlation between the optical luminosity of a quasar and the submm emission from its quasar host galaxy using samples of radio-quiet, optically loud quasars at $z > 4$ and $z \approx 2$ (Isaak et al. 2002; Priddey et al. 2003). What is striking, however, are the detections at both $850\mu m$ and $450\mu m$ of SDSS1148+5251.

It is not possible to fit the two fluxes reported here and the 1.2mm flux with a single-temperature SED parameterised by $T_d = 40$, and $\beta = 2$ (see Figure 1: solid line). A better fit can be achieved, with a much hotter characteristic dust temperature $T_d = 180\text{K}$, and $\beta = 0$ (Figure 1: dotted line), or using a two-component model with a cool component characterised by $T_d = 40\text{K}; \beta = 0$ and a hotter component with $T_d = 140\text{K}; \beta = 1.5$. However, we stress that there are insufficient data points to constrain such a two-component

model. If, in the first instance, we assume that the underlying SED is indeed best characterised by a single-temperature, then there are a number of different factors that need to be explored to establish the origin of the anomalous flux ratios, which can be broadly grouped into those that result in an anomalously high millimetre flux, and those that may result in systematically low submm fluxes. However, it is clear that observations with a higher signal-to-noise are urgently needed in order to better constrain the model fitting. Furthermore, the high photometric precision of ALMA, of order a few percent, will be crucial for future analyses of this type.

3.2.1 A high 1.2mm flux:

If we assume that the observed $850\mu m$ flux is correct, then there are a number of observational and physical reasons why the observed 1.2mm and $450\mu m$ fluxes might deviate from values expected for a single-temperature SED model:

Relative calibration: Calibration at mm and long-submm wavelengths is relatively straightforward, particularly under periods of high and stable atmospheric transmission. A comparison of calibrators common to JCMT and IRAM by Lisenfeld and collaborators suggests that the calibrator fluxes measured at $850\mu m$ and 1.2mm are consistent with thermal SED profiles. We have included calibration errors of 10 – 15% in our plotted rms estimates. Accurate calibration at $450\mu m$, however, is far more difficult with small, temporal variations in atmospheric extinction, (τ), contributing significantly to the final, overall flux. We estimate that the combined random and systematic error in the individual flux measurements to be about 30%. We have included calibration errors in the error-bars plotted in Figure 1, calculated by taking the square root of the sum of the squares of the different error components.

Synchrotron contamination: Synchrotron emission can contribute significantly to the observed mm fluxes of radio-loud quasars, with boosting from either the synchrotron tail in the quasar itself, or from a source in its neighbourhood. VLA observations at 43GHz by Bertoldi et al. (2003) place a $S(3\sigma)_{43\text{GHz}} < 0.33\text{mJy}$

on radio emission from the quasar at 43GHz. This strongly suggests that the 1.2mm emission is thermal rather than non-thermal given the positive spectral shape. A search of the NVSS (Condon et al. 1998) and FIRST (Becker et al. 1995) radio catalogues did not reveal any radio sources within a 30 arcsec radius of the optical position of the quasar. The FIRST survey has a 0.138mJy/beam rms at the quasar position (1.4GHz), which places a 3σ upper limit to the synchrotron contamination of the 1.2mm flux by radio sources in the quasar field of 0.5mJy, based on the worse case of a flat-spectrum radio source.

Lensing: Gravitational lensing can boost observed flux measurements considerably (eg. F10214+4724 (Broadhurst & Lehar 1995), APM 08279+5255 (Irwin et al. 1998; Ibata et al. 1999)). In general, however, the magnification is achromatic. Thus, all (sub)mm fluxes would be scaled by the same factor unless the physical extent of the regions emitting at the different wavelengths were quite different – for example, if the mm flux ($\lambda_{rest} = 170\mu\text{m}$) traced a cooler and, most importantly, highly extended region whilst the shorter wavelength emission traced much more compact emission. It is not possible to establish this, however, without the high spatial resolution achievable using mm interferometers.

Spectral line contamination: Line contamination of submm continuum fluxes observed in local galaxies is widely recognised. Observations by Zhu et al. (2003) have shown that the CO(3–2) rotational line can contribute as much as 70% to the 850 μm continuum flux. At $z \sim 6.43$ the CO(3–2) ($\lambda_{rest} = 867\mu\text{m}$) line is redshifted to 6.46mm (46.4GHz), well outside the 1.2mm and 850 μm filter passbands. Under good observing conditions, the 1.2mm filter has an effective pass-band of around 80GHz, which at $z \sim 6.43$ includes the forbidden, rest-frame far-infrared (FIR) transition of C^+ ($\lambda_{rest}=157.74\mu\text{m}$). Significant flux boosting by this line is, however, unlikely: observations with ISO have shown that the line-to-FIR ratio in local starbursts and ULIRGs (Luhman et al. 1998, 2003) is a factor of ten or more lower than that seen in normal galaxies (0.1–1%: (Stacey et al. 1991)). If we assume an equivalent filter width of the MAMBO-2 camera at 1.2mm of around 80GHz, then the C^+ line peak would need to be over 500mJy to account for the excess emission at 1.2mm(1.3mJy) above that expected for a single-temperature SED fit. This would be equivalent to a line contribution to the FIR luminosity of about 1%. A search by Isaak et al. (1994) for the redshifted C^+ emission line in the optically-luminous, radio-quiet quasar BR B1202–0725 at $z = 4.695$ placed a 3σ upper limit of $\sim 1.8 \times 10^{-4}$ on the line contribution to the FIR luminosity (equivalent to a 3σ upper limit to the line of $\sim 60\text{mJy}$, and to the line-to-continuum ratio of just over 1 in a line-width of 250kms^{-1}) in this, the most submm-bright of the $z > 4$ quasars. Thus, whilst an intriguing possibility, it is unlikely that contamination by C^+ is responsible for the high 1.2mm flux.

3.2.2 A low 850 μm flux:

If, in contrast, we assume that the 1.2mm flux is correct, then the observed submm fluxes at 850 μm and 450 μm are a factor of 1.4 and 0.7 lower than one would expect from a single-temperature, $T_d = 40\text{K}; \beta = 2$ SED fit. The 850 μm detection flux is at $> 10\sigma$ and as such is, at first glance, almost 4σ below the single temperature fit derived from the 1.2mm flux. The statistical significance of the difference however, ranges between $0.7 < \frac{S_{850}^{est} - S_{850}^{obs}}{\sigma_{850}^{obs}} < 6.7$ where S_{850}^{est} is the 850 μm flux estimated from the observed 1.2mm flux when one factors in the uncertainties in the 1.2mm flux and the error bars in the SED fit itself. The statistical significance of the

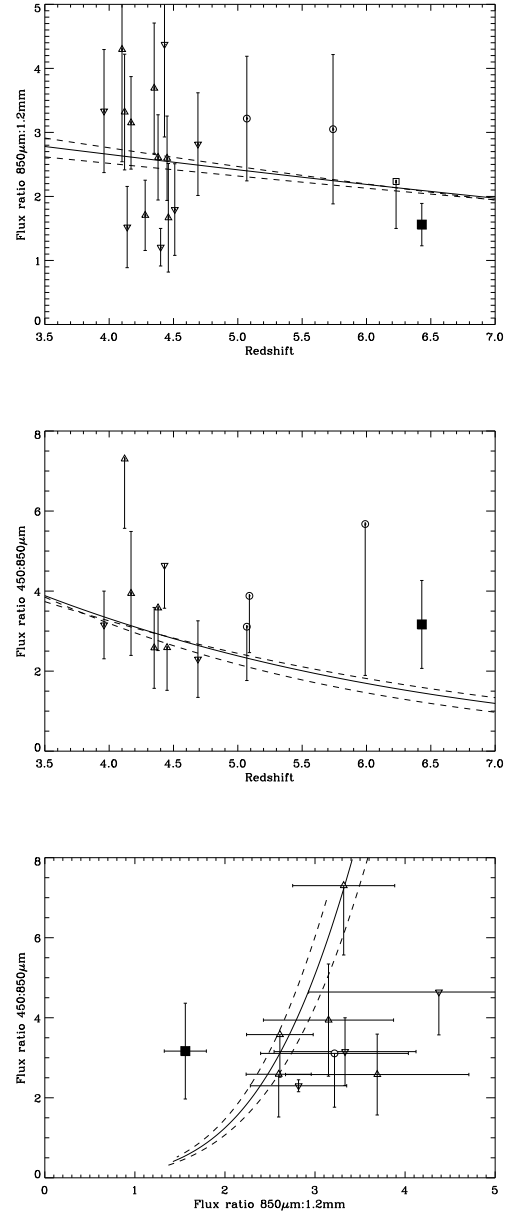


Figure 2. Mm and submm flux ratios: diagnostics of the underlying SEDs.

Upper panel: Ratio of $S_{850\mu\text{m}}/S_{1.2\text{mm}}$ as a function of redshift

Middle panel: Ratio of $S_{450\mu\text{m}}/S_{850\mu\text{m}}$ as a function of redshift

Lower panel: Ratio of $S_{450\mu\text{m}}/S_{850\mu\text{m}}$ vs. $S_{850\mu\text{m}}/S_{1.2\text{mm}}$

In each case the solid and dashed lines represent the locus of the ratios calculated from the Priddey&McMahon SED and 1σ deviations therefrom respectively; the upright triangles represent data taken from Isaak et al., (in prep.); the inverted triangles data taken from Omont et al. (1996); McMahon et al. (1999); Omont et al. (2001); Carilli et al. (2001); Isaak et al. (2002); Bertoldi et al. (2003), the open circles data taken from Priddey et al. 2003b and the filled square the detection reported in this paper. The error bars are 1σ values. The anomalous observed fluxes can best be seen in the lower panel, where the ratio of the ratios deviates by between 1 and 3σ from the single-temperature SED fit.

difference between the observed and predicted $450\mu\text{m}$ flux is much less, as the detection itself is only at 3σ . Interestingly, the discrepancy between the observed $450\mu\text{m}$ flux and that derived from the 1.2mm flux (scale factor of 3.3 from Figures 2a–c) is smaller.

Thus, the observations of SDSS1148+5251 suggest that the dust emission is not well characterised by a single-temperature SED fit. One cannot, however, attach high significance to this statement because of the relatively low value of the signal-to-noise at $450\mu\text{m}$ in particular. Bearing this in mind there is *very tentative* evidence that alludes to a change in the properties of the high- z quasar hosts with redshift. There is a considerable spread in the flux ratios and a more detailed analysis of the SEDs requires not only very high signal-to-noise data in the $450\mu\text{m}$ filter, but also data taken at even shorter wavelengths that match more closely the peak and predicted turnover of the rest-frame SED. We defer a more detailed discussion of the SEDs of high- z quasars, as well as tentative trends with redshift to Isaak et al. (in prep.)

3.3 Inferred properties

SDSS1148+5251 is unique for two reasons: first, on account of its redshift; second, because it is detected not only at 1.2mm and $850\mu\text{m}$, but, uncommonly for a high-redshift quasar, also at $450\mu\text{m}$. The consequence of assuming a low T_d —as suggested by the 1.2mm– $850\mu\text{m}$ flux ratio—is a prohibitively large dust mass. This burdens us with explaining how so much dust synthesis could have taken place without the formation redshift being unacceptably high. If, in contrast, T_d is high—as suggested by the 450 – $850\mu\text{m}$ ratio—there is no problem accounting for the dust mass, which is small as a result. This is, however, at the cost of a large FIR luminosity. Indeed, if the dust really is this hot, then the far infrared luminosity approaches the blue luminosity of the quasar, which would suggest that reprocessed AGN emission is not the dominant mechanism heating the dust.

Notwithstanding the uncertainty in dust temperature, Table 2 lists the properties all the targets would have if they were “average” $z > 4$ quasars, i.e. possessing the $T_d=40\text{K}$ and $\beta=2$ fit by Priddey & McMahon (2001). The cosmological parameters $\Omega_M=0.3$, $\Omega_\Lambda=0.7$, $H_0=65\text{km/s/Mpc}$ are assumed. $t(\infty) - t(z)$ is the difference in look-back time between redshift z and redshift ∞ . As in Priddey et al. (2003b) we adopt a dust opacity of $\kappa(\lambda)=30\text{cm}^2\text{g}^{-1} \times \lambda^{-2}$ M_d is thus the mass of dust. $\dot{M}_*(\text{min})$ is the absolute minimum sustained star formation rate needed to synthesise M_d within the available time. M_{bh} and \dot{M}_{acc} are the black hole mass and accretion rate calculated from the absolute B magnitude (M_B) assuming Eddington accretion (eg. Isaak et al. (2002)). We have, however, shown that observed submm emission from SDSS1148+5251 is not consistent with the Priddey et al. (2001) fit. In Figure 1 we have considered instead a selection of alternative SEDs: the “hot” model ($T_d=180\text{K}$, $\beta=0$) has $(L_{FIR}, M_d)=(1.1 \times 10^{14} L_\odot, 0.3 \times 10^8 M_\odot)$, whilst the two-component model illustrated has $(L_{FIR}, M_d)=(2.9 \times 10^{14} L_\odot, 3.3 \times 10^8 M_\odot)$. The “mean” SED, on the other hand, gives $(L_{FIR}, M_d)=(0.1 \times 10^{14} L_\odot, 5.3 \times 10^8 M_\odot)$.

4 CONCLUSIONS

The rest-frame FIR spectral energy distribution is key to determining the thermal origin of the observed submm emission from high-redshift quasars. The observations presented here suggest that the

host galaxies of quasars out to redshifts of $z > 6$ are actively undergoing star formation. Multi-wavelength observations spanning the mm and submm are crucial to providing constraints on the dust mass, far-infrared luminosity and inferred star formation rate, thus further exploring the role of star formation in high-redshift quasar host galaxies.

ACKNOWLEDGMENTS

We would like to thank staff at JCMT and JAC for their support during observing, along with the referee who responded extremely promptly and with helpful suggestions.

REFERENCES

- Becker R.H., White R.L., Helfand D.J., 1995, ApJ, 450, 559
 Bertoldi F., Carilli C.L., Cox P., Fan X., Strauss M.A., Beelen A., Omont A., Zylka R., 2003, A&A, 406, L55
 Broadhurst T., Lehar J., 1995, ApJ, 450, L41
 Carilli C.L. et al., 2001, ApJ, 555, 625
 Condon J.J., Cotton W.D., Greisen E.W., Yin Q.F., Perley R.A., Taylor G.B., Broderick J.J., 1998, AJ, 115, 1693
 Fan X. et al., 2003, AJ, 125, 1649
 Gebhardt K. et al., 2000, ApJ, 539, L13
 Holland W.S. et al., 1999, MNRAS, 303, 659
 Iyata R.A., Lewis G.F., Irwin M.J., Lehar J., Totten E.J., 1999, AJ, 118, 1922
 Irwin M.J., Iyata R.A., Lewis G.F., Totten E.J., 1998, ApJ, 505, 529
 Isaak K.G., McMahon R.G., Hills R.E., Withington S., 1994, MNRAS, 269, L28
 Isaak K.G., Priddey R.S., McMahon R.G., Omont A., Cox P., Peroux C., Sharp R., 2002, MNRAS, 329, 149
 Jenness T., Lightfoot J., 1998a, in ASP Conf. Ser. 145: Astronomical Data Analysis Software and Systems VII
 Jenness T., Lightfoot J., 1998b, in Starlink User Note 216
 Jenness T., Economou F., 1999, in ASP Conf. Ser. 172: Astronomical Data Analysis Software and Systems VIII The SCUBA Data Reduction Pipeline: ORAC-DR at the JCMT
 Luhman M.L., Satyapal S., Fischer J., Wolfire M.G., Cox P., Lord S.D., Smith H.A., Stacey G.J., Unger S.J., 1998, ApJ, 504, L11
 Luhman M.L., Satyapal S., Fischer J., Wolfire M.G., Strum E., Dudley C.C., Lutz D., Genzel R., 2003, ApJ, 594, 758
 McMahon R.G., Omont A., Bergeron J., Kreysa E., Haslam C.G.T., 1994, MNRAS, 267, L9
 McMahon R.G., Priddey R.S., Omont A., Snellen I., Withington S., 1999, MNRAS 309, L1
 Omont A., McMahon R.G., Cox P., Kreysa E., Bergeron J., Pajot F., Storrie-Lombardi L.J., 1996, A&A, 315, 1
 Omont A., Cox P., Bertoldi F., McMahon R.G., Carilli C., Isaak K.G., 2001, A&A, 374, 371
 Priddey R.S. & McMahon R.G., 2001, MNRAS, 324, L17
 Priddey R.S., Isaak K.G., McMahon R.G., Omont A., 2003a, MNRAS, 339, 1183
 Priddey R.S., Isaak K.G., McMahon R.G., Robson E.I., Pearson C.P., 2003b, MNRAS, 344, L74
 Stacey G.J., Geis N., Genzel R., Lugten J.B., Poglitsch A., Sternberg A., Townes C.H., 1991, ApJ, 373, 423
 Zhu M., Seauquist E.R., Kuno N., 2003, ApJ, 588, 243

This paper has been typeset from a $\text{\TeX}/\text{\LaTeX}$ file prepared by the author.